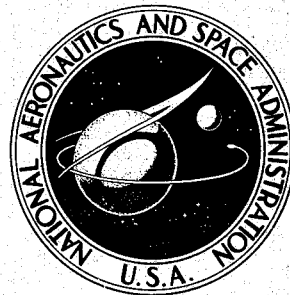


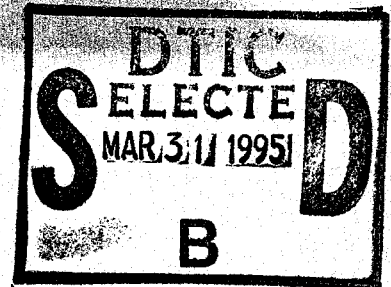
**NASA TECHNICAL  
MEMORANDUM**



NASA TM X-3104

NASA TM X-3104

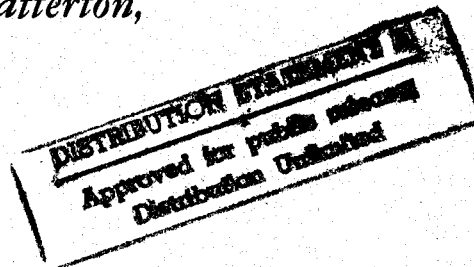
19950329 087



**TERMINAL-SHOCK AND RESTART CONTROL  
OF A MACH 2.5, MIXED-COMPRESSION INLET  
COUPLED TO A TURBOFAN ENGINE**

*by Robert J. Baumbick, Peter G. Batterton,  
and Carl J. Daniele*

*Lewis Research Center  
Cleveland, Ohio 44135*



NATIONAL AERONAUTICS AND SPACE ADMINISTRATION • WASHINGTON, D. C. • AUGUST 1974

DTIC QUALITY INSPECTED 1

1. Report No. NASA TM X-3104	2. Government Accession No.	3. Recipient's Catalog No.	
4. Title and Subtitle TERMINAL-SHOCK AND RESTART CONTROL OF A MACH 2.5, MIXED-COMPRESSION INLET COUPLED TO A TURBOFAN ENGINE		5. Report Date August 1974	6. Performing Organization Code
		8. Performing Organization Report No. E-7924	
7. Author(s) Robert J. Baumbick, Peter G. Batterton, and Carl J. Daniele		10. Work Unit No. 501-24	11. Contract or Grant No.
9. Performing Organization Name and Address Lewis Research Center National Aeronautics and Space Administration Cleveland, Ohio 44135		13. Type of Report and Period Covered Technical Memorandum	
		14. Sponsoring Agency Code	
12. Sponsoring Agency Name and Address National Aeronautics and Space Administration Washington, D.C. 20546		15. Supplementary Notes	
16. Abstract  Results of an experimental program conducted on a mixed-compression inlet coupled to a turbofan engine are presented. Open-loop frequency response data are presented that show the response of shock position (as measured by an average inlet static pressure) to sinusoidal airflow disturbances produced at the compressor face station. Also presented are results showing the effect of different passive terminations (a choke plate or a long duct) on the characteristics of the inlet. Transfer functions obtained by using experimental data are presented and compared to the experimental data. Closed-loop frequency response of shock position (with a proportional-plus-integral controller) is presented. In addition, transient data are presented that show the unstart-restart characteristics of the inlet.			
17. Key Words (Suggested by Author(s)) Supersonic inlet - engine control Supersonic inlet dynamics Mixed-compression inlets		18. Distribution Statement Unclassified - unlimited Category 28	
19. Security Classif. (of this report) Unclassified	20. Security Classif. (of this page) Unclassified	21. No. of Pages 18	22. Price* \$3.00

\* For sale by the National Technical Information Service, Springfield, Virginia 22151

TERMINAL-SHOCK AND RESTART CONTROL OF A MACH 2.5,  
MIXED-COMPRESSION INLET COUPLED TO A TURBOFAN ENGINE

by Robert J. Baumbick, Peter G. Batteredton, and Carl J. Daniele

Lewis Research Center

SUMMARY

Open-loop frequency response data are presented that show the response of shock position (as measured by an average inlet static pressure) to sinusoidal air-flow disturbances at the compressor face station. These data are for the inlet alternately coupled to a choked orifice, a long duct, and an engine. The frequency response data were obtained by sinusoidally varying bypass area. The bypass doors were located at a point just upstream of the compressor face station. Closed-loop frequency response data and time history traces of inlet variables are also presented.

Data are presented to show controlled inlet unstart-restart transient phenomena with the engine operating. These data also show the effect of the terminal-shock controller gain on the shock position stability during a restart cycle. The inlet was unstarted by momentarily closing off the centerbody bleed of the inlet.

The response of the control pressure to airflow disturbances for the inlet coupled to an operating turbofan engine was similar to that obtained by using a long-duct termination but did not show the same well defined resonances in the higher frequency range. The absence of the resonances for the inlet-engine combination is attributed to the damping effect produced by the fan stages of the engine and instrumentation in the fan duct (pressure rakes, etc.).

A proportional-plus-integral controller was used for terminal-shock control because it gave zero steady-state error and desirable low-frequency attenuation. The terminal-shock controller gains had to be reduced during an inlet restart because of the increased gain of the inlet during the restart cycle.

## INTRODUCTION

Overall propulsion system efficiency is in part determined by inlet pressure recovery and by the distortion levels at the compressor face. Supersonic, mixed-compression inlets are designed to provide maximum pressure recovery and low distortion levels when the terminal shock is located slightly downstream of the geometric throat of the inlet. Any displacement of the shock from this point has an adverse effect upon propulsion system performance. Upstream displacement results in an inlet unstart. Downstream displacement results in lower pressure recovery and higher distortion. If the distortion is sufficiently high, the compressor will be driven into stall. Terminal-shock control is needed to counteract any disturbance which would move the terminal shock from the desired operating point. In addition, in the event of an inlet unstart, some method must be available to restart the inlet automatically and return the shock to its operating point.

One method of providing terminal-shock control is to manipulate overboard bypass doors located in the inlet diffuser as a function of some inlet variable which is indicative of terminal-shock position. Some previous work done in developing high-response terminal-shock controls by using overboard bypass doors is reported in references 1 and 2.

A test program was conducted in the Lewis 10- by 10-foot supersonic wind tunnel on a mixed-compression inlet coupled to a turbofan engine. The inlet was designed for operation at Mach 2.5, and 45 percent of the supersonic area contraction occurred internally. The engine was a low-bypass-ratio turbofan engine (TF-30-P3). This program was the first one in which a mixed-compression-inlet - turbofan-engine combination was run at Lewis. Results from a previous program in which a mixed-compression-inlet - turbojet-engine combination was run are reported in reference 3.

The portion of the test program described in this report deals primarily with the inlet and considers the engine as an active termination. These tests supplement previous tests conducted on this inlet with the inlet coupled to passive terminations such as a choked orifice or a long duct. The results from the previous program are reported in reference 2.

Results are presented in the form of frequency domain plots showing the effect of the engine on the open-loop terminal-shock-position frequency response. Closed-

loop frequency response of the control variable is also presented. Results in the form of time histories of selected inlet variables are presented for inlet unstart-restart cycles.

### SYMBOLS

- A area,  $\text{cm}^2$
- f frequency, Hz
- M Mach number, dimensionless
- P total pressure,  $\text{N/cm}^2$
- p static pressure,  $\text{N/cm}^2$
- s Laplace operator, 1/sec
- T temperature, K
- V volume,  $\text{cm}^3$
- $\zeta$  damping ratio, dimensionless
- $\omega$  frequency, rad/sec
- Subscripts:
- c corner frequency
- cl cowl lip
- n natural frequency
- to total temperature
- tt total pressure at inlet throat
- 23, ..., 66 distance in centimeters from cowl lip
- Superscript:
- average value

Accession For	
NTIS GRA&I	<input checked="" type="checkbox"/>
DTIC TAB	<input type="checkbox"/>
Unannounced	<input type="checkbox"/>
Justification	
By _____	
Distribution/	
Availability Codes	
Dist.	Avail and/or Special
A-1	

## APPARATUS, INSTRUMENTATION, AND PROCEDURE

### Apparatus

The tests were conducted in the Lewis 10- by 10-foot supersonic wind tunnel. The propulsion system tested combined a mixed-compression inlet with an after-burning turbofan engine. All tests were conducted at the following average free-stream conditions: Mach number, 2.5; total temperature, 297 K; total pressure, 9.3 newtons per square centimeter; Reynolds number index, 0.86; and specific-heat ratio, 1.4. The propulsion system was operated at zero angle of attack during all the controls tests.

The inlet, designed at Lewis, is an axisymmetric, mixed-compression inlet with a translating spike centerbody and 45-percent internal supersonic area contraction (fig. 1). The inlet is designed for Mach 2.5 operation with a TF-30 engine. The inlet has a capture area of 7070 square centimeters and measures 180 centimeters from the cowl lip to the fan face. Provisions are made for boundary-layer bleed on the centerbody and cowl. For this program the inlet cowl bleeds were sealed. The centerbody bleed is a slot type bleed. The flow is ducted to four equally spaced struts located in the diffuser section and is controlled by a butterfly valve in each strut. The butterfly valves are positioned by electrohydraulic servovalves having vane type hydraulic motor actuators.

The inlet is equipped with eight slotted-plate overboard bypass doors used to match inlet-engine airflow. Figure 2 shows a view of the inlet diffuser section which indicates the location of the bypass doors and the centerbody bleed flow struts. The even numbered doors were used for disturbance, and the odd numbered doors were used as control doors in the terminal-shock control system. Each odd numbered door has an open area of 404 square centimeters for a linear motion of 2.54 centimeters. Each even numbered door has an open area of 50.5 square centimeters for the same linear displacement. Detailed information on the bypass doors used in this test program is presented in reference 4. Reference 5 contains detailed information on the design of the electrohydraulic servosystem.

## Instrumentation

Linear motion of the bypass doors is measured by linear variable differential transformers (LVDT's). This measuring system has negligible dynamics in the frequency range covered during these tests (0.1 to 100 Hz). Figure 3 is a sketch of the inlet showing the positions of the steady-state pressure transducers used to indicate terminal-shock location. These 16 transducers start 23 centimeters from the cowl lip and extend to a point 66 centimeters from the cowl lip. The 14 transducers farthest upstream are spaced 2.54 centimeters apart. The last two transducers are spaced 5.08 centimeters apart. Steady-state terminal-shock position was measured by defining the supersonic static-pressure profile measured by the transducers. The output from the transducers was connected to a cathode-ray-tube display in the control room. The terminal-shock location was determined by noting which static-pressure transducer was the first to read a higher level than the supersonic value.

The transient pressures were measured with strain-gage transducers connected to the cowl through short tubes. The pressure measuring system had negligible dynamics in the frequency range covered in these tests. The transient pressure transducers are located in a plane 66 centimeters from the cowl lip (fig. 3). There are four transducers spaced  $90^\circ$  apart in this plane. The four pressures in this plane were averaged electrically to obtain an average pressure identified as  $\bar{p}_{66}$ .

In addition to the transducers just discussed, high-response pressure transducers were used to measure total pressure at the inlet throat  $P_{tt}$  and a static pressure on the cowl near the inlet lip  $p_{cl}$ .

## Data Acquisition and Reduction

Frequency response data were taken on magnetic tape (FM system) using sweep frequency techniques. The data were then reduced off line on a computer by the methods described in reference 6. Frequency response data are presented as normalized amplitude ratios (normalized to the 0.1-Hz value). Transient data were recorded on two eight-channel strip-chart recorders.

## RESULTS AND DISCUSSION

### Terminal-Shock Dynamics and Control

The response of inlet shock position (as measured by an average static pressure  $\bar{p}_{66}$ ) to downstream airflow disturbances (produced by varying bypass area) is shown in figure 4. The responses shown in this figure are for the inlet - choke-plate, inlet - long-duct, and inlet-engine combinations. The responses for the passive terminations (choke plate and long duct) were obtained from a previous program (ref. 2). The data indicate that the responses for the engine and long-duct terminations are quite similar out to about 15 hertz. The lower corner frequency for the long duct and engine is attributed to the added volume of the long duct and to the volume of the fan duct and the afterburner of the engine. Beyond the 15-hertz point the inlet-engine combination response shows more attenuation than the inlet - long-duct combination. This additional damping is attributed to the fan stages of the engine and to the instrumentation in the fan duct.

When data from the inlet - long-duct combination and an expression derived from reference 7 were used, the first-order corner frequency was calculated to be 3.21 hertz (20.2 rad/sec). When the volumes for the engine fan duct and afterburner section were used, the corner frequency was calculated to be 3.61 hertz (22.71 rad/sec). The expression used for calculating the first-order corner frequency (in hertz) is

$$f_c = \frac{2.21 A_{ex} \sqrt{T_{to}}}{V} \quad (1)$$

where  $A_{ex}$  is the total exit area (in square meters) including the bypass area,  $T_{to}$  is the total temperature, and  $V$  is the equivalent volume of the inlet and long duct or of the fan duct and afterburner (in cubic meters).

In order to illustrate the effect of damping on the response of the inlet-engine combination shown in figure 4, the experimental data for both the inlet - long-duct and inlet-engine combinations were fed into a frequency domain curve fit program. This program requires an initial guess at the structure of the transfer function and uses a quadratic cost function to optimize the values of the parameters. The transfer-function expressions obtained for the inlet - long-duct and inlet-engine responses shown in figure 4 are as follows:

Inlet and long duct:

$$\bar{p}_{66} = \frac{\left[ \left( \frac{s}{99} \right)^2 + \frac{2(0.419)s}{99} + 1 \right] \left[ \left( \frac{s}{295} \right)^2 + \frac{2(0.086)s}{295} + 1 \right]}{\left( \frac{s}{19} + 1 \right) \left[ \left( \frac{s}{185} \right)^2 + \frac{2(0.31)s}{185} + 1 \right] \left[ \left( \frac{s}{343} \right)^2 + \frac{2(0.168)s}{343} + 1 \right] \left[ \left( \frac{s}{433} \right)^2 + \frac{2(0.66)s}{433} + 1 \right]} \quad (2)$$

Inlet and engine:

$$\bar{p}_{66} = \frac{\left[ \left( \frac{s}{51} \right)^2 + \frac{2(0.62)s}{51} + 1 \right] \left[ \left( \frac{s}{364} \right)^2 + \frac{2(0.019)s}{364} + 1 \right]}{\left( \frac{s}{24} + 1 \right) \left( \frac{s}{24} + 1 \right) \left( \frac{s}{194} + 1 \right) \left[ \left( \frac{s}{383} \right)^2 + \frac{2(0.061)s}{383} + 1 \right] \left[ \left( \frac{s}{433} \right)^2 + \frac{2(0.44)s}{433} + 1 \right]} \quad (3)$$

The structure for both combinations is the same, but the values of the parameters have been changed to fit the data. Equations (2) and (3) are in terms of first- and second-order frequency functions. The first-order terms are written as  $1 + s/\omega$ , and the second-order terms are written as  $1 + 2(\zeta)s/\omega_n + (s/\omega_n)^2$ . In these expressions  $\omega$  and  $\omega_n$  are in radians per second,  $\zeta$  represents the damping number, and  $s$  is the Laplace operator. In both expressions the first-order fill time effect is evident and is represented by the simple poles. For the long duct the pole is at 19 radians per second (compared to a calculated value of 20.2 rad/sec), and for the engine the pole is at 24 radians per second (compared to a calculated value of 22.71 rad/sec). The complex pole with  $\omega_n = 185$  radians per second (29.5 Hz) for the long duct has been changed to two simple poles for the engine. This change was made because the experimental data showed a significant damping effect for the inlet-engine combination. Figure 5 shows normalized amplitude ratios for experimental data and transfer-function approximations for both combinations being discussed. The agreement between experimental data and the transfer function is quite good for both cases. The experimental phase data, not shown, result in a similar fit with the transfer function.

In figure 6 a sketch of the inlet terminal-shock and restart control system is shown. The restart control system is discussed in the next section. The terminal-shock control system measures the average throat exit static pressure  $\bar{p}_{66}$  (which is

indicative of shock position) and compares it with a desired value. The error between the two values is then passed through the control filter, and the resulting signal is used to position the control bypass doors to move the terminal shock back to its operating point and thereby reduce the error to zero.

A proportional-plus-integral control filter was used because it resulted in zero steady-state error, provided desirable low-frequency attenuation, and was a simple structure to implement. Figure 7 shows a comparison of the open- and closed-loop frequency responses for the inlet-engine combination. The closed-loop response crosses the open-loop response at approximately 4.7 hertz. Beyond this point the closed-loop response is higher than the open-loop response up to 60 hertz, at which point the controller becomes inactive and the response open-loop. In terms of terminal-shock motion figure 7 indicates that in the low-frequency range below 4.7 hertz the closed-loop control inhibits terminal-shock excursions considerably.

### Restart Control

The restart control (fig. 6) functions when the terminal shock is expelled from the inlet and it unstarts. When the inlet unstarts, two things happen: (1) the spike (centerbody) is commanded to extend to increase the ratio of throat to cowl lip area to permit reswallowing of the shock, and (2) a pressure command which is a complex function of centerbody position is switched into the terminal-shock-position controller to prevent inlet buzz and to prevent the terminal shock from operating too supercritically after the inlet is restarted but before the spike is on design.

The ratio of cowl lip static to throat total pressure  $p_{cl}/P_{tt}$  is used for the unstart sensor. When the ratio exceeds a reference value, the inlet is considered to be in the unstarted mode, and the restart procedure, just defined, is initiated. The pressure ratio is low when the inlet is started because the cowl lip static pressure is low (is measured in the supersonic flow region) and the throat total pressure is high (as a result of the high inlet recovery). When the inlet unstarts, the pressure ratio is high. The cowl lip static pressure is high because the cowl lip pressure is in the subsonic flow region, and the total pressure is low because of the lower inlet recovery.

Figure 8 shows selected inlet variables during an inlet unstart-restart cycle.

The following discussion describes the sequence of events identified by the numbers with the curves in the figure. The inlet is unstarted by momentarily closing off the centerbody bleed flow with the strut valves. After the disturbance is applied, the terminal shock moves upstream ( $\bar{p}_{66}$  rises slightly) (1). The control doors attempt to compensate by opening, but the inlet unstarts (2). At this time the pressure  $\bar{p}_{63}$  drops to its unstarted value (pressure recovery is low) (3). Also, the spike is commanded to extend (4), and the unstarted pressure command is switched into the terminal-shock control system (5). The unstarted pressure command is a complex function of spike position and was determined from a manual restart procedure. Implementation of this function is accomplished with analog comparators and relays. When the spike reaches a point where the throat to cowl lip area ratio is right for the restart (6), the spike is commanded to return to its design position (7). During the restarted portion of the transient an instability occurred in the terminal-shock control loop (8) (20-Hz oscillations). These oscillations resulted from the high gain of the inlet during restart. This instability was subsequently corrected.

Figure 9 shows an unstart-restart cycle that is similar but shows the effect of reduced terminal-shock controller gain. The gain was reduced by a factor of 4 as soon as there was an indication of an unstart and was not returned to normal until the inlet was restarted and the spike was back on design. In both figures 8 and 9 the disturbance doors (small area) were set to a fully open position when the inlet unstarted and remained open from then on. The control doors, therefore, were reset to a different steady-state value.

## SUMMARY OF RESULTS

Results are presented showing the effect of an operating turbofan engine on the characteristics of the inlet pressure used in the terminal-shock control system. The results indicate that the engine and long-duct terminations have the same effect on the inlet in the frequency range below 15 hertz. Beyond this frequency the results from the inlet-engine combination show considerably more attenuation than those from the inlet - long-duct combination. The low-frequency effect can be attributed to the fill time required for the engine fan duct and afterburner volume. The resonances produced with the long-duct termination do not show up when the inlet is

coupled to the engine. The response of the inlet-engine combination shows more attenuation beyond the 15-hertz point. This additional damping is attributed to the engine fan stages and to the instrumentation in the fan duct (pressure rakes, etc.). The results obtained indicate that there might be some coupling between the engine and inlet and that disturbances produced by the engine, such as afterburner light offs, may well reflect up into the inlet. Further investigation in this area is necessary.

The inlet was successfully controlled by using a proportional-plus-integral control function. This type of control results in zero steady-state error and desirable low-frequency attenuation and is a simple structure to implement. The results presented show that the closed-loop frequency response crosses the open-loop response at approximately 4.7 hertz.

It was necessary to use a complex pressure command signal for the shock controller during the restart cycle to prevent inlet buzz and also to prevent the terminal shock from operating too supercritically during inlet restart. In addition, the results presented show the need for reducing the terminal-shock controller gains during the restart cycle to prevent an instability in the shock position control loop.

Lewis Research Center,  
National Aeronautics and Space Administration,  
Cleveland, Ohio, April 4, 1974,  
501-24.

#### REFERENCES

1. Cole, Gary L; Neiner, George H; and Baumbick, Robert J: Terminal Shock Position and Restart Control of a Mach 2.7, Two-Dimensional, Twin-Duct Mixed-Compression Inlet. NASA TM X-2818, 1973.
2. Baumbick, Robert J.; Wallhagen, Robert E.; Neiner, George H.; and Batterton, Peter G.: Dynamic Response of a Mach 2.5 Axisymmetric Inlet with 40 Percent Supersonic Internal Area Contraction. NASA TM X-2833, 1973.

3. Neiner, George H.; Crosby, Michael J.; and Cole, Gary L: Experimental and Analytical Investigation of Fast Normal Shock Position Controls For a Mach 2.5 Mixed-Compression Inlet. NASA TN D-6382, 1971.
4. Webb, John A., Jr.; Mehmed, Oral; and Hiller, Kirby W.: Improved Design of a High-Response Slotted-Plate Overboard Bypass Valve for Supersonic Inlets. NASA TM X-2812, 1973.
5. Zeller, John R.; and Webb, John A., Jr.: Determination and Evaluation of Performance Limit Criteria of Fast-Response Electrohydraulic Servosystems. NASA TM X-2736, 1973.
6. Milner, Edward J.; and Bruton, William M.: Application of a Hybrid Computer to Sweep Frequency Data Processing. NASA TM X-2753, 1973.
7. Bowditch, David N.; and Wilcox, Fred A.: Dynamic Response of a Supersonic Diffuser to Bypass and Spike Oscillation. NASA TM X-10, 1959.

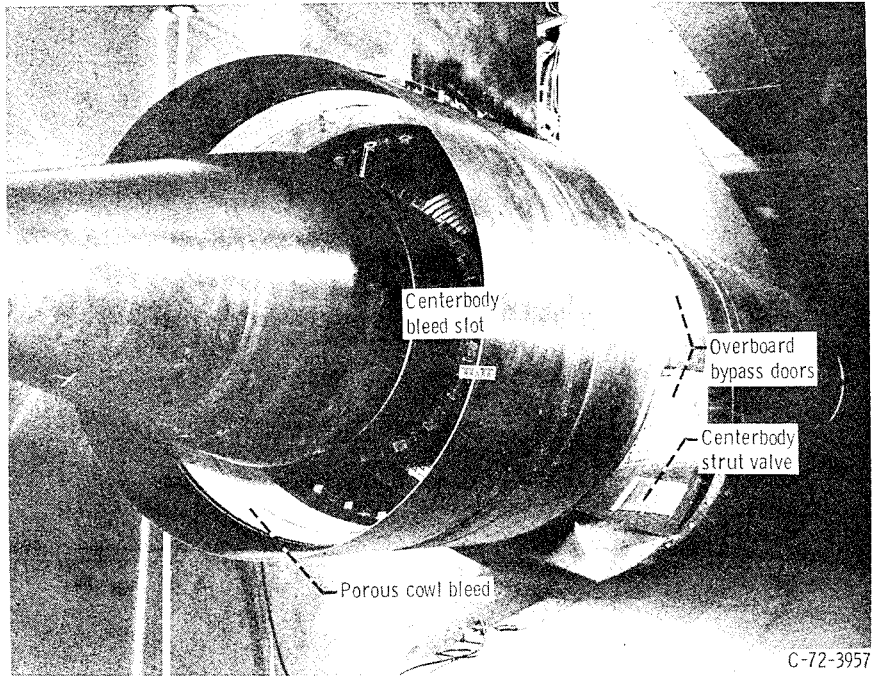


Figure 1. - Inlet installed in test section.

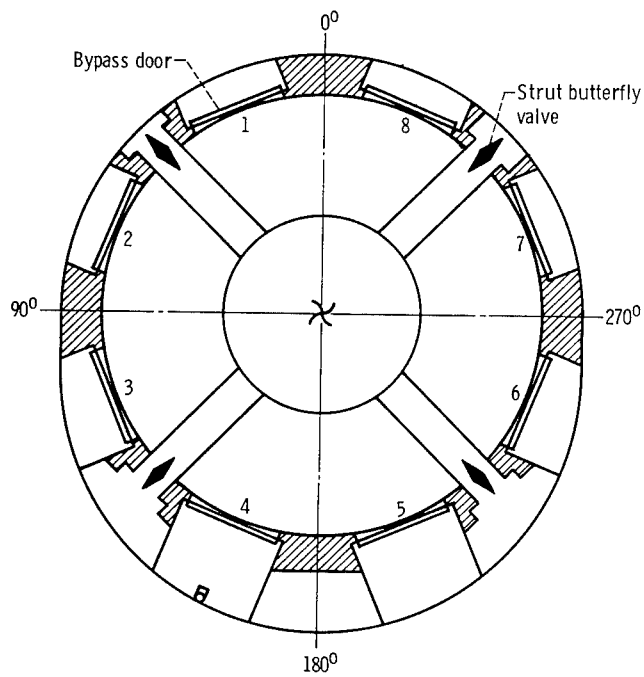


Figure 2. - View of inlet diffuser looking downstream showing bypass doors and centerbody bleed flow struts.

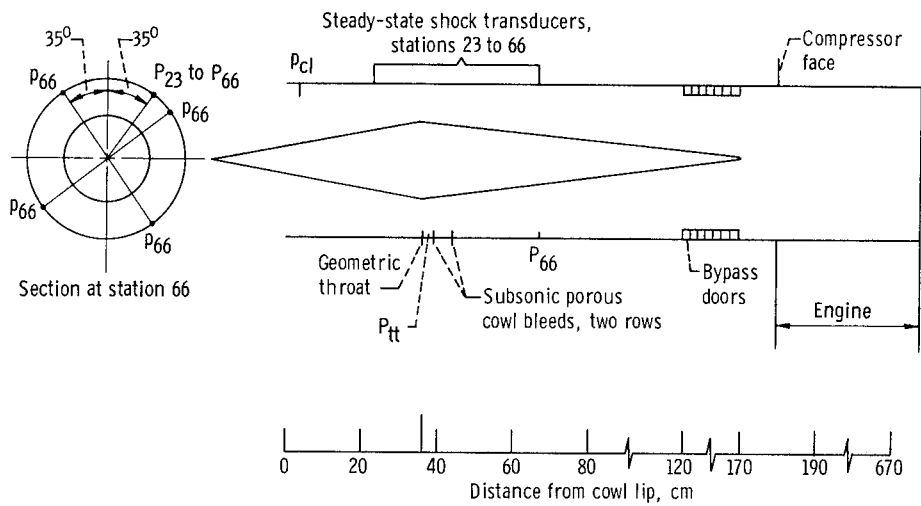


Figure 3. - Location of steady-state and dynamic instrumentation on inlet.

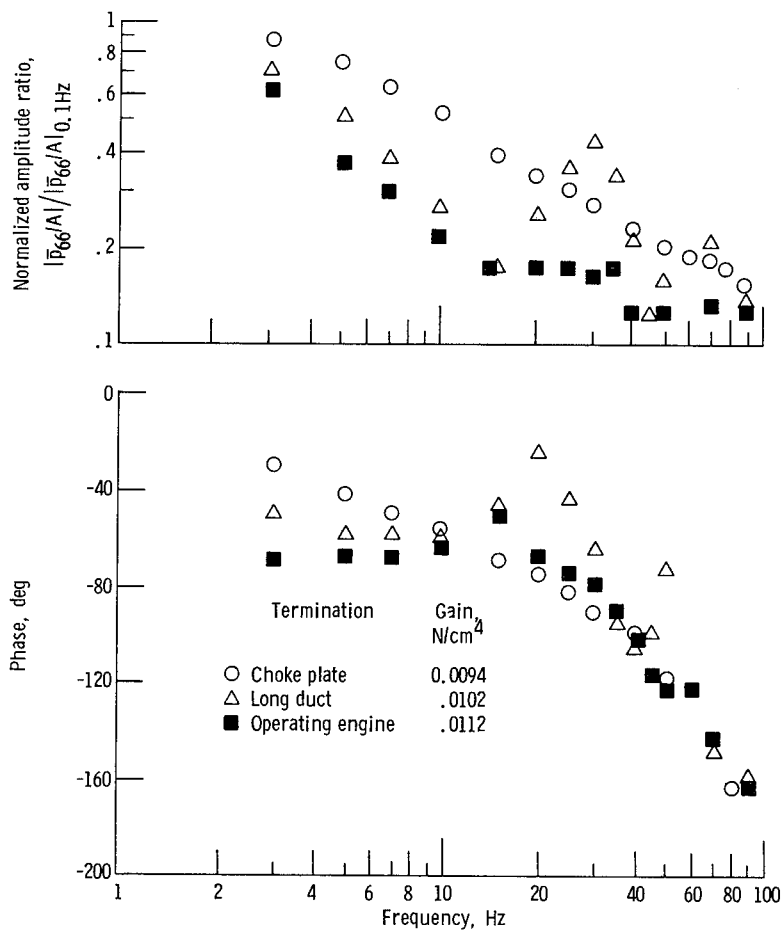


Figure 4. - Normalized amplitude ratio and phase plots of inlet pressure at Mach 2.5. No cowl bleed; long duct and operating-engine terminations.

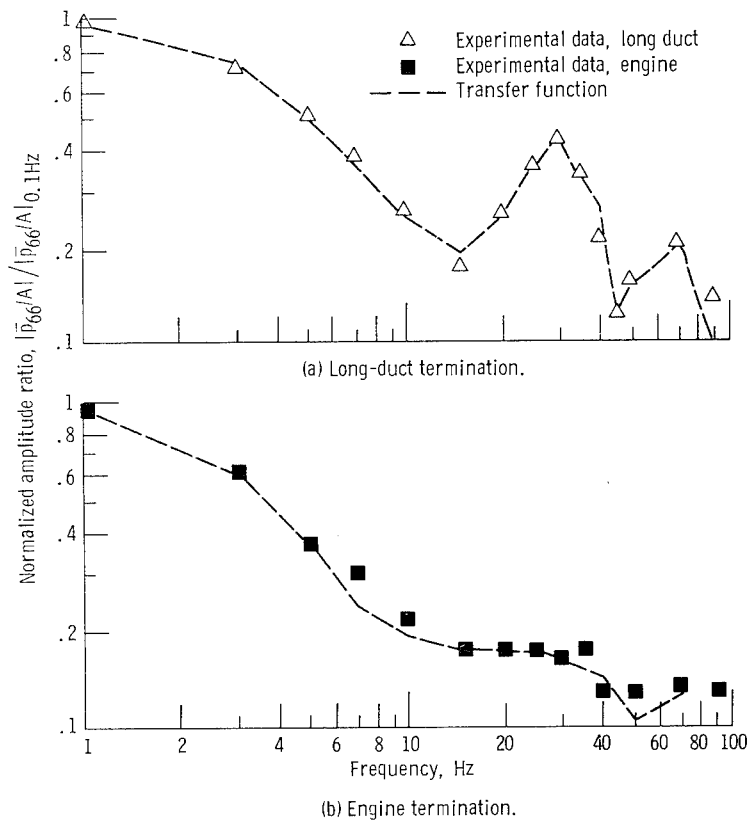


Figure 5. - Experimental normalized amplitude ratio of inlet pressure and transfer-function approximation to data.

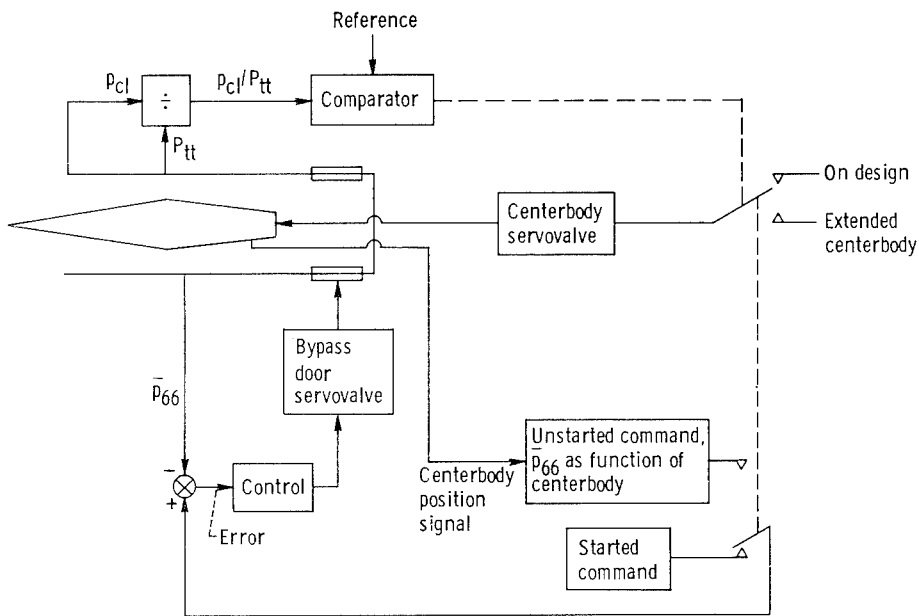


Figure 6. - Sketch of terminal-shock control and restart control systems for inlet.

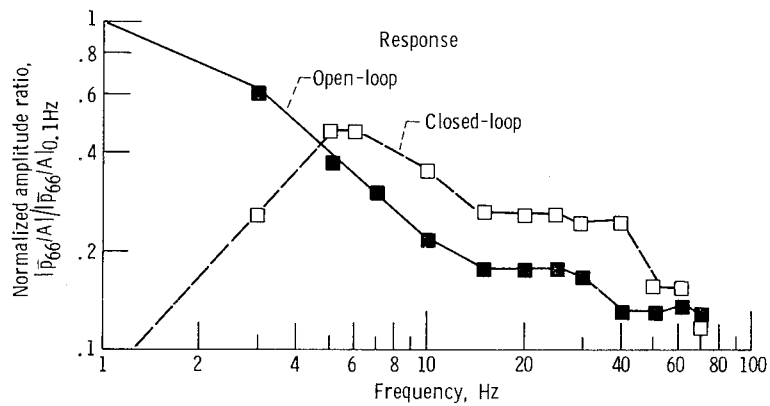


Figure 7. - Open- and closed-loop response of inlet pressure for Mach 2.5 conditions. No cowl bleed; inlet coupled to operating engine.

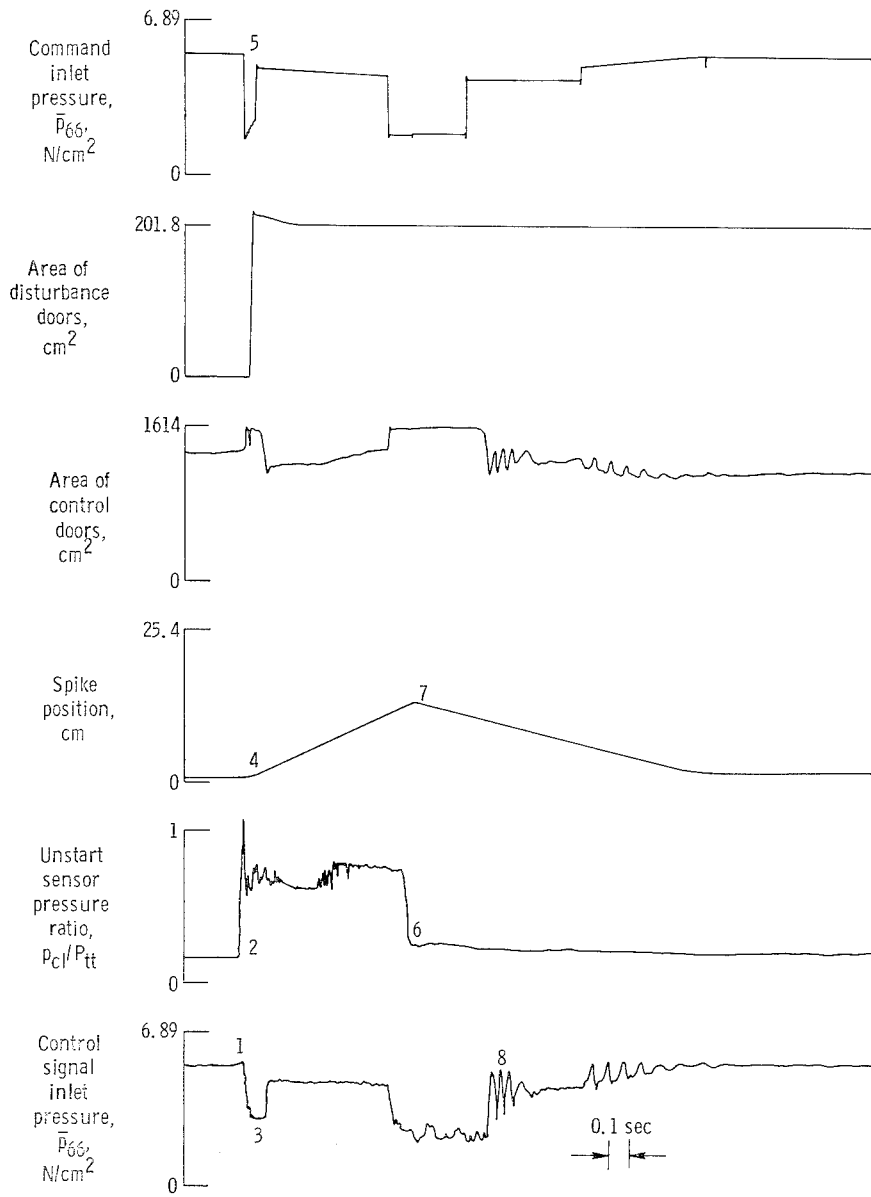


Figure 8. - Inlet unstart-restart cycle with nominal terminal-shock controller gains for Mach 2.5 conditions.

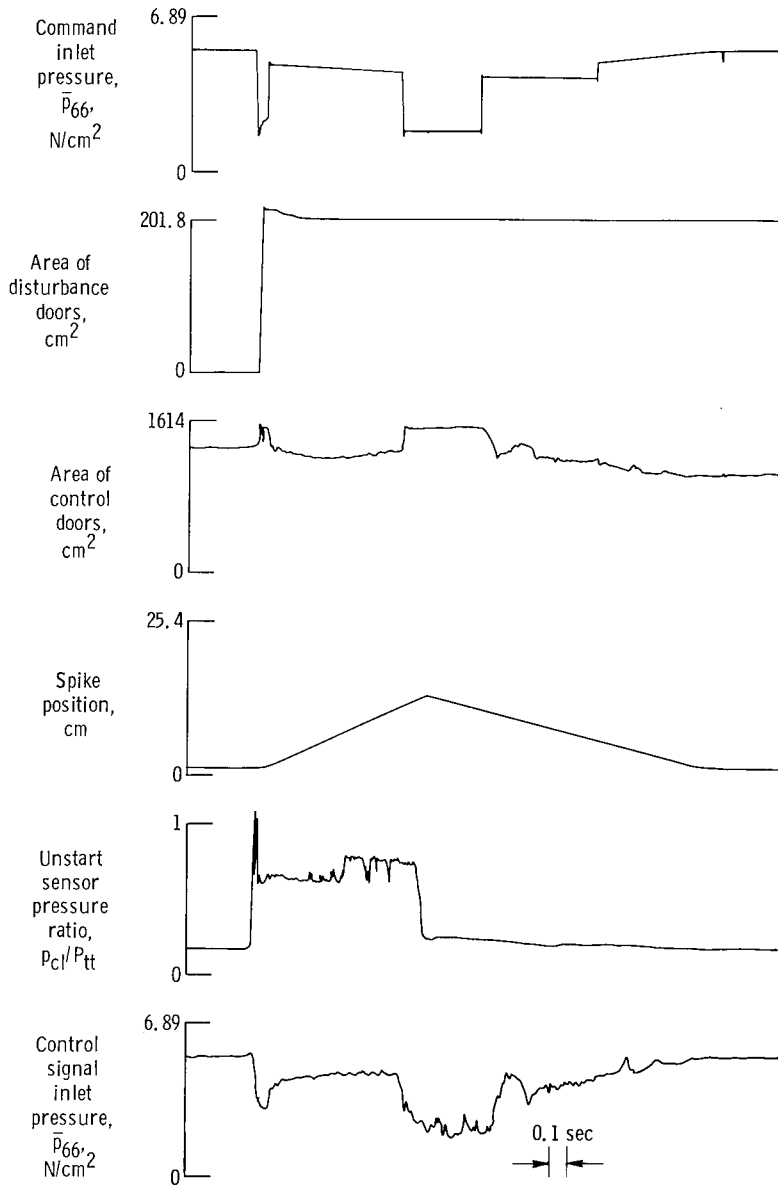


Figure 9. - Inlet unstart-restart cycle with reduced terminal-shock controller gains for Mach 2.5 conditions.